

*Supplement of*

## **Droplet activation behaviour of atmospheric black carbon particles in fog as a function of their size and mixing state**

Ghislain Motos<sup>1</sup>, Julia Schmale<sup>1</sup>, Joel Christopher Corbin<sup>1,\*</sup>, Marco Zanatta<sup>1,\*\*</sup>, Urs Baltensperger<sup>1</sup> and Martin Gysel<sup>1</sup>

<sup>1</sup>Laboratory of Atmospheric Chemistry, Paul Scherrer Institute, 5232 Villigen PSI, Switzerland

\*Now at Measurement Science and Standards, National Research Council Canada, 1200 Montreal Road, Ottawa K1A 0R6, Canada

\*\*Now at Alfred Wegener Institute, Helmholtz Centre for Polar and Marine Research, Bremerhaven, Germany

*Correspondence to:* Martin Gysel (martin.gysel@psi.ch)

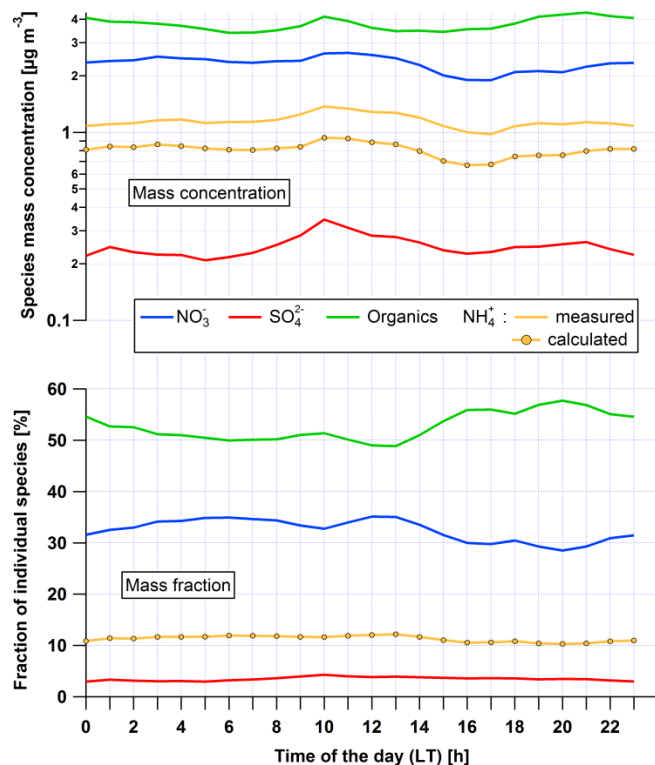


Figure S1:Top: Diurnal variations of mass concentrations measured by the ACSM (top) and corresponding mass fractions (bottom) for the full campaign duration from 6 November 2015 to 31 January 2016. The maximum expected  $\text{NH}_4^+$  mass concentration, calculated with assuming that all particulate  $\text{NO}_3^-$  and  $\text{SO}_4^{2-}$  was neutralized by  $\text{NH}_4^+$  and that no other anions were present in substantial fraction (i.e.  $n(\text{NH}_4^+) = 2 \cdot n(\text{SO}_4^{2-}) + n(\text{NO}_3^-)$ ), is shown as a dotted line. The measured  $\text{NH}_4^+$  mass concentration was higher than this maximum calculated concentration; however, the difference is within measurement uncertainty. Mass fractions of organic matter and salts shown in the bottom panel are based on this calculated maximum  $\text{NH}_4^+$  mass concentration.

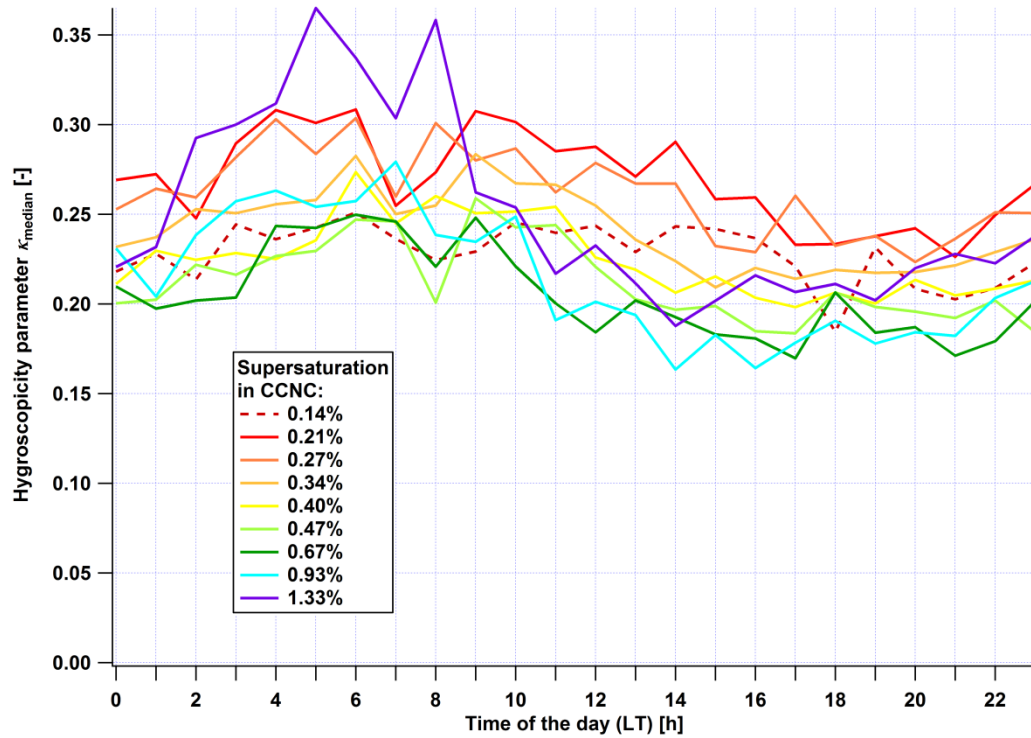
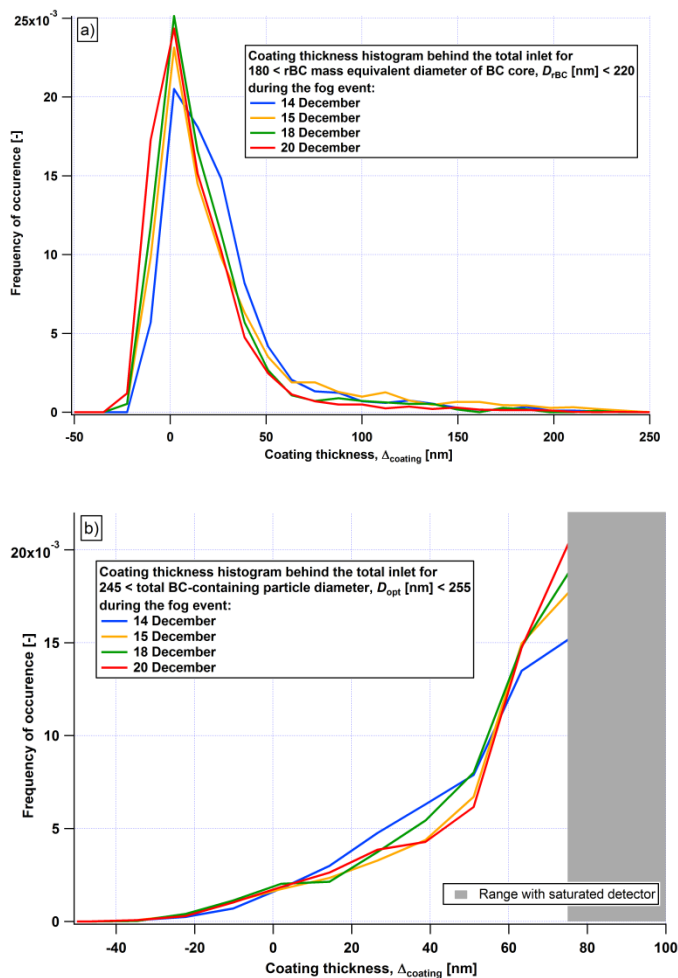


Figure S2: Diurnal patterns of the hygroscopicity parameter  $\kappa_{\text{median}}$  extracted from sCCNC measurement and separately averaged by SS for the whole campaign. Dashed line style is used for 0.14 % and 1.33 % supersaturation due to higher CCNC calibration uncertainty compared to the other supersaturations.



**Figure S3: Histograms of BC coating thickness normalized by the area during the analysed fog events for a fixed BC core diameter range (a) and a fixed total particle diameter range (b).**

Figure S3a shows a histogram of the coating thickness of BC cores with a mass equivalent diameter ( $D_{rBC}$ ) of  $200 \pm 20$  nm during every fog event analysed. Occurrence of negative coating thickness values, which is derived from independent light scattering and incandescence signals, can have two reasons. First, random noise in the single particle signals causes random noise around the true value in derived single particle coating thickness values. Accordingly, a negative coating thickness will be assigned to half of the uncoated BC cores, however, this is not an issue as the mean coating thickness reported for a particle ensemble will not be biased. Second, systematic calibration biases or inappropriate assumptions the simplified optical model including refractive indices used to interpret the raw signal can potentially introduce a systematic positive or negative bias in reported coating thickness values. Such potential bias is minimized by comparing the sizing of single BC cores from their incandescence signal (mass-equivalent diameter) and their scattering signal (optical diameter) and ensuring the close agreement between these two quantities. The four histograms in Figure S3a are very similar and show that the dominant fraction of BC-containing particles possess a relatively thin coating, with histograms peaking close to 0 nm (bare BC). This type of analysis, which is relevant for BC core size and thus also BC core mass weighted properties, shows that fresh or recently emitted BC particles dominate over aged BC particles contributed by the background aerosol.

Figure S3b also shows histograms of coating thickness for each fog event analysed, but in this case including all BC-containing particles with an overall particle optical diameter between 245 nm and 255 nm (as opposed to filtering by similar BC core size as done in in Figure S3a). Again, there is very little variability between the fog events. Here, we find that the dominant fraction of BC cores is thickly coated. The conclusions extracted from these two types of histograms seem to be contradictory but the number size distribution of BC cores (Fig. S4) explains in parts why it is not: BC-containing particles at a fixed overall particle size include either large BC cores without coating or small BC cores with thick coating (or something in between), whereas neither small uncoated BC cores nor large coated BC cores are included. Figure S3b shows that, even at this urban site, a BC-containing particle with a certain overall particle size is more likely to be from background aerosol (thick coating and thus small BC core) than a freshly emitted traffic BC particle (uncoated and thus large BC core). This seems to be in contradiction to the results shown in, however, the number size distribution of BC cores shown in Figure S4 explains why this is not in contradiction to the results shown in Figure S3a as the number size distribution peaks way below  $D_{\text{rBC}} = 100$  nm and drops steeply between  $D_{\text{rBC}} = 100$  nm and 250 nm. Therefore, small aged BC cores are more abundant than large fresh BC cores despite BC mass being dominated by fresh emissions.

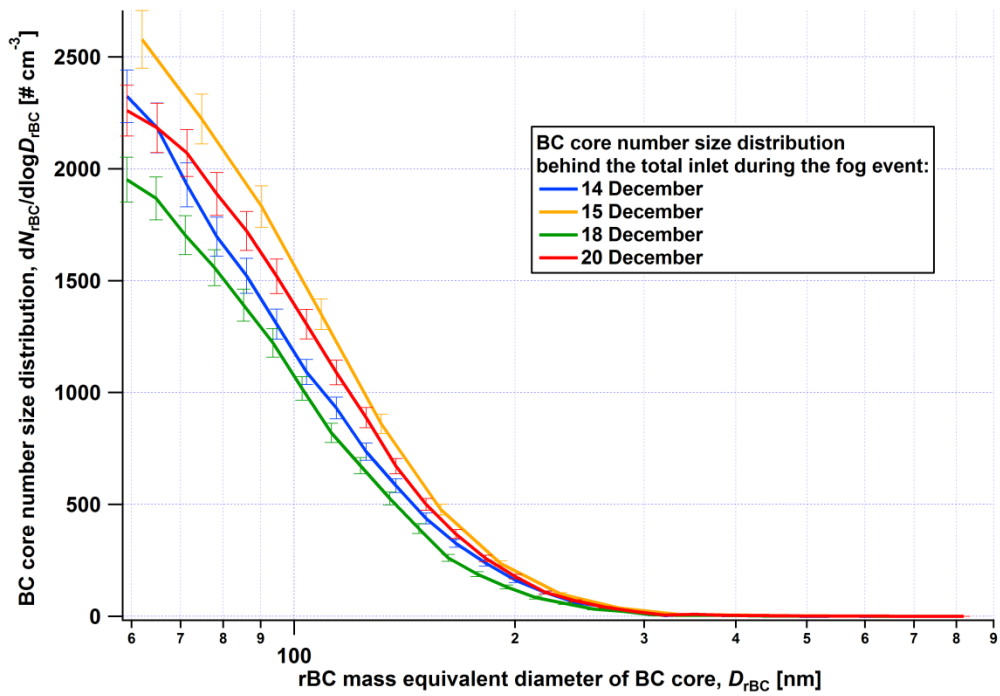
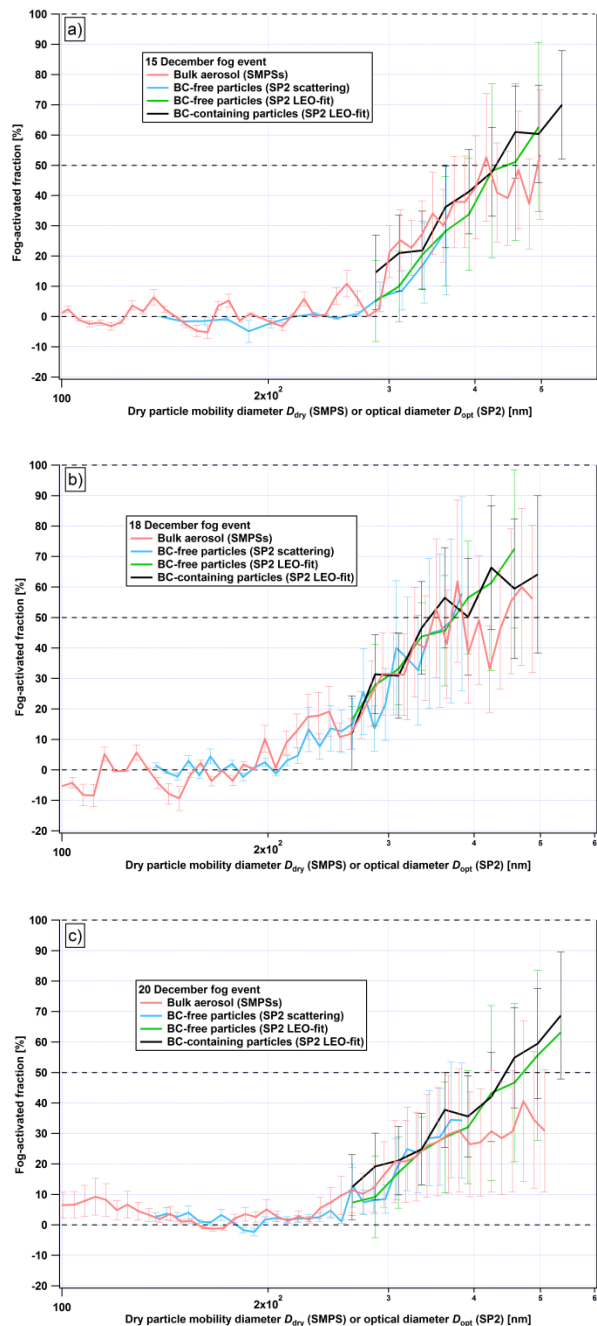


Figure S4: Number size distribution of BC cores during the analysed fog events.



**Figure S5: Activated fractions of the bulk aerosol (SMPS, red lines) BC-containing (SP2, black lines) and BC-free particles (SP2 scattering analysis, blue line and LEO-fit analysis, green lines) during the 15 (a), 18 (b) and 20 (c) December fog events. The 1- $\sigma$  uncertainties of the BC-containing particle data are Poisson-based with respect to the BC core number size distribution; the other ones are dominated by the level of (dis-)agreement of the interstitial and total measurements, which was determined during out-of-cloud periods and propagated through the calculation of activated fraction.**